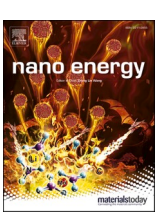


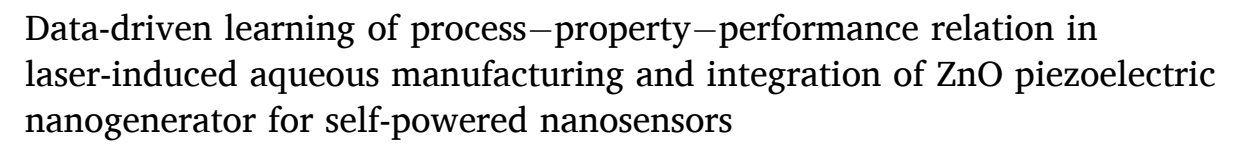
Contents lists available at ScienceDirect

Nano Energy

journal homepage: http://www.elsevier.com/locate/nanoen



Communication





- ^a School of Industrial Engineering, Purdue University, West Lafayette, IN 47907, USA
- ^b Flex Laboratory, Purdue University, West Lafayette, IN 47907, USA
- ^c Birck Nanotechnology Center, Purdue University, West Lafayette, IN 47907, USA

ARTICLE INFO

Keywords: Nanomanufacturing Data-driven learning Process—property—performance relationship Piezoelectric nanogenerator Zinc oxide nanowires

ABSTRACT

Piezoelectric nanogenerators have attracted intensive interest in harvesting the stray mechanical energy in the environment to power miniaturized electronics and sensors. However, their efficient integration into systems and compatibility with existing technologies for practical applications remains challenging. Here, we report for the first time the systematic, data-driven learning of the process-property-performance relation in ZnO nanowires piezoelectric nanogenerators that are synthesized and integrated through a laser-induced chemical process. An experiment-derived behavioral model was established to reveal the apparent connections between the production parameters and the output performance of the ZnO piezoelectric nanogenerator. We further demonstrated the application of such knowledge for integrating the optimized ZnO nanowires piezoelectric nanogenerator with a photosensor into a self-powered sensor system, exhibiting the potential for future system-level improvements.

1. Introduction

Harvesting energy from the ambient environment could enable effective and sustainable pathways for powering the operations of electronics [1-4]. Diverse technologies have been demonstrated [5-8] for scavenging a broad spectrum of environmental energies to enable self-powered systems. Among these technologies, the piezoelectric nanogenerator (PENG) [2,9] can convert the otherwise wasted mechanical energy abundant in the environment. Various piezoelectric nanogenerators have been developed based on nanostructured piezoelectric materials such as zinc oxide (ZnO) [2], gallium nitride (GaN) [10], lead zirconate titanate (PZT) [11], and polyvinylidene fluoride (PVDF) [12]. To this end, ZnO nanomaterials attracted the most attention for biocompatibility [13,14] and the feasibility in deriving high-quality crystals through facile synthesis [15–18]. Among various preparation methods of ZnO nanostructures, laser technology provides a facile approach to grow ZnO nanowires on arbitrary patterns and even on the non-flat, 3D curved surfaces by scanning a focused laser beam as a local heat source in a fully digital manner [19]. The localized heating of laser also enables the high growth rates that are orders of magnitude higher than those of conventional hydrothermal methods with bulk heating [20], indicating the ability of laser-induced method for efficient manufacturing of nanostructures. In addition, the laser-induced deposition could occur in an aqueous system, which is much safer and cheaper than a vacuum environment or a gas environment with high temperatures required by the general deposition methods [19]. Hence, the laser-induced method is promising for scalable manufacturing of nanostructures with precise control.

In recent years, numerous efforts have been devoted to improving the performance of ZnO-based PENGs, regarding their flexibility [21], outputs [22], and stability [23] to meet the requirements of applications in areas such as wearable devices [24] and biomedical engineering [25]. Nevertheless, the process-property-performance relation critical for the scalable manufacturing and integration of ZnO-based PENGs is yet to be identified in state-of-the-art research. Designing and fabricating nanodevices that can be integrated into a functional system is essential for translating nanoscale science into applicable nanotechnology [26]. In an ideal case, the desirable performance of nanodevices could be determined by the applications and achieved by controlling the fabrication parameters. However, the relationships between performances and fabrication parameters are not always straightforward. Although theoretical models and simulations have been made available for PENGs [27,

^{*} Corresponding author at: School of Industrial Engineering, Purdue University, West Lafayette, IN 47907, USA. *E-mail address:* wenzhuowu@purdue.edu (W. Wu).

28], the actual behaviors of PENGs are likely to deviate from the predicted/simulated scenarios. Rigorous statistical analysis can enable the development of the behavioral model that connects the observed performances with the production parameters. Based on the limited available experimental data, the impacts of the production parameters on the device performance can be estimated and learned through regression analysis. Such behavioral models can lead to a comprehensive understanding of the process-property-performance relation, which can guide the design of the production process for targeted performance, and the improvements on production yield, uniformity, and quality of the integrated nanosystems [29].

Here, we demonstrate for the first time the data-driven learning of the process-property-performance relation in the laser-induced aqueous synthesis and integration of ZnO PENG through statistical analysis. ZnO nanowires arrays were produced by a room-temperature laser-induced chemical deposition, which prepares ZnO nanowires arrays at predefined locations with good control of the nanowire density and morphology [30,31]. The as-prepared ZnO nanowires arrays were further integrated into PENGs and electrically characterized. A behavioral model was estimated to reveal the apparent effects of growth parameters. The optimized ZnO PENG, suggested by this model, was further demonstrated and integrated with a nanowire-based photosensor for demonstrating the operation of a self-powered sensor system. The knowledge obtained from this study could guide the future design, manufacturing, and optimization of ZnO PENGs. The technical approach demonstrated in this work can also be applied to the optimized production and integration of other nanodevices.

2. Results and discussion

ZnO nanowires were synthesized using laser-induced chemical deposition with controlled density and morphologies. Laser-induced synthesis provides unique opportunities for customized applications through growing nanomaterials locally with the controlled morphology in a precise and effective manner. A pulsed laser is employed in this work because it offers more degrees of freedom in the parameter space for controlling and tuning the growth of nanomaterials, compared to the

continuous-wave laser. The density and morphology control of ZnO nanowires by pulsed laser was studied kinetically and thermodynamically in previous works [30,31]. The control of nanowire density could be realized by decoupling the nanowire growth process from ZnO nucleation on new sites [30]. Different morphologies of ZnO nanowires could be obtained by adjusting the laser power density [31]. Therefore, the controlled density and morphologies were achieved through carefully selecting the combinations of laser power density, growth time, amount of added acid, and other experimental conditions. The growth parameters of ZnO nanowires, including growth density, length, and diameter, are holistically designed to involve all possible combinations of growth parameters' levels. Leveraging the tunable pulsed laser, we can grow the ZnO nanowires arrays on seedless silicon wafers. Fig. 1a-fshow some typical scanning electron micrographs of the ZnO nanowires arrays with various growth densities, diameters, and lengths. The growth area can be determined by the laser spot whose radius was fixed at 200 µm for all ZnO nanowires arrays, which can be further enlarged by increasing the laser beam size. The measured lengths and diameters are summarized in Fig. 1g and 1h, respectively, with fitting distributions represented by the red lines.

To investigate ZnO PENG's output performances, we integrated the as-deposited ZnO nanowires arrays into piezoelectric devices. The scheme of the fabrication is shown in Fig. 2a. The silicon substrate used for ZnO nanowires growth was employed as the bottom electrode. The as-grown ZnO nanowires were fully covered by a dielectric layer of polydimethylsiloxane (PDMS) between the top and bottom electrodes. The PDMS was spin-coated with 3000 rpm/min for 5 min. The thickness of the PDMS layer was about 10 µm [32], larger than the maximum length of ZnO nanowires to ensure full coverage. A silver-paste electrode was added on top of the PDMS layer as the top electrode. An external force was applied vertically to the silicon substrate along the c-axis of ZnO nanowires. As shown in Fig. 2b, the ZnO nanowires were compressed when the force was applied, and a piezoelectric potential was generated between the top and bottom surfaces by the relative displacement of the Zn^{2+} cations with respect to the O^{2-} anions [2]. Due to the existence of the dielectric layer between ZnO top surfaces and the top electrode, the generated piezoelectric charges on the top surfaces

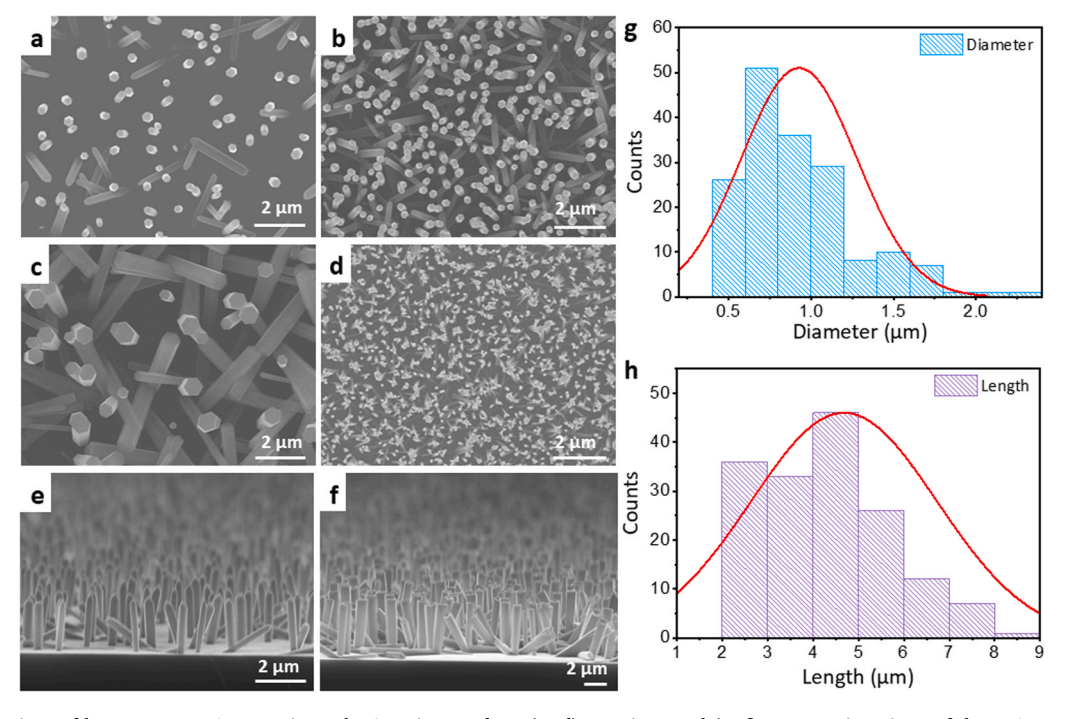


Fig. 1. Characterizations of laser-grown ZnO nanowires. The SEM images from (a-d) top views and (e-f) cross-section views of the ZnO nanowires arrays with various growth densities, diameters, and lengths. The distributions of the measured (g) diameters and (h) lengths of ZnO nanowires.

R. Wang et al. Nano Energy 83 (2021) 105820

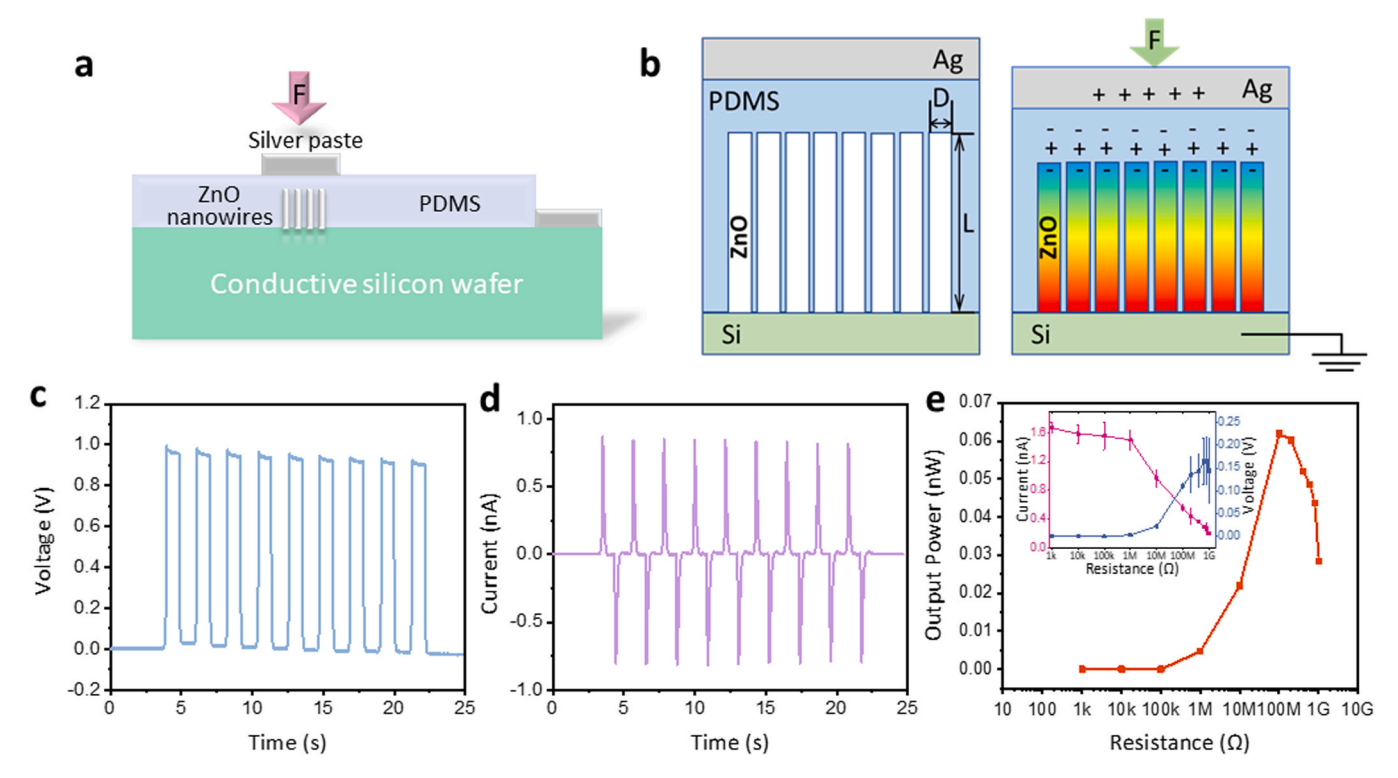


Fig. 2. (a) The scheme of the fabrication structure of a ZnO nanowires piezoelectric nanogenerator. (b) Modeling of a ZnO nanowires array undergone a compressive force. The typical output (c) voltage and (d) current generated from a ZnO nanowires piezoelectric nanogenerator. (e) The output power dependence on the resistance of the external load. Inset: the voltage and current curves with different resistors.

would electrostatically induce charges in the top electrode, which drives the transient flow of free electrons in the external circuit. When the force was released, the electrons flowed back, and the system returned to an equilibrium state. A dynamically applied force hence resulted in the periodic outputs. The typical PENG output data is shown in Fig. 2c and d. We further connected different load resistances from 1 $K\Omega$ to 1 $G\Omega$ in the external circuit to characterize the output power. The measured currents, voltages, and calculated power are summarized in Fig. 2e. The measured maximum instantaneous output power density was about 0.477 mW/m^2 for a 200 μm -radius laser synthesis. All prepared ZnO nanowires arrays and related PENGs were characterized and analyzed using the above method.

Regression analysis is a widely used statistical methodology for modeling the relationships between a response variable y and a vector of explanatory variables X [29,33]. In our case, the collected PENG output data was utilized as the response variable to build up the connection with the growth parameters. The analytical expression of output y as a function of growth parameters can therefore be written as:

$$y = f(L, D, DE) \tag{1}$$

where L and D are the geometric parameters (Fig. 2b). L and D are the length and diameter of a ZnO nanowire, and DE is the density of a ZnO nanowire array. Apart from the length and diameter, the aspect ratio (AR = L/D) was considered as an effective parameter to quantify the geometric morphologies of ZnO nanowires [28]. To examine whether the length and diameter would influence the outputs independently or collectively, we included the aspect ratio (AR) as one of the potential variables. In addition, from Coulomb's law, the electrostatic induction becomes weaker with a longer distance [34]. Thus, with the existence of the dielectric layer, the measured outputs are directly related to the induced charges in the electrodes, which are smaller than the generated piezoelectric charges due to the attenuation of electrostatic induction. The thickness of PDMS layers among all devices was fixed to be 10 μ m. The distance between the top electrode and the top surfaces of ZnO

nanowires can be estimated by r = 10 - L, which is the linear combination of length. The expression of outputs can thus be written as

$$= f(L, D, DE, AR) \tag{2}$$

The collected data (180 points) was imported into analytical software (SAS®) for subsequent analysis. The scatter matrix was plotted to understand the relationships among variables (Fig. S1). Some obvious outliers were observed and removed. The outliers could be due to deviations in the fabrication conditions, unsuccessful control of the growth parameters, and systematic error during the tests. After this initial screening process, there were 170 data points ready for use in the model fitting. A strong correlation exists between the measured voltages and currents, where the values of currents are proportional to those of voltages (Fig. 3a). Hence, to simplify the model, we selected current as the only variable of interest. After that, linear regression models were employed to analyze these data. From the scatter matrix, it can be seen that none of the regressors has linear relationships with the current. The box-cox procedure was applied to suggest a possible transformation of the response variable. The λ determined by the log-likelihood function was between 0 and 0.5, suggesting the logarithmic or square-root transformations (Fig. 3b). After testing and evaluating the two transformations, respectively, the logarithmic transformation was selected due to the better fitting performances. Therefore, the logarithmic transformation on the response variable (PENG current) was performed in all following models. The possible combinations of the regressors and their transformations were tested through the stepwise-regression selection to automatically select a set of variables that nicely fit the data. The selected model can be expressed as

Outputcurrent =
$$c * AR^{0.798} * e^{1.91DE} * \frac{e^{1.538D}}{e^{0.141L}}$$
 (4)

where c is a coefficient related to the material properties, AR, DE, D, and L are the measured aspect ratio, density, diameter, and length, respectively. The estimated parameters and the analysis of variance (ANOVA)

R. Wang et al. Nano Energy 83 (2021) 105820

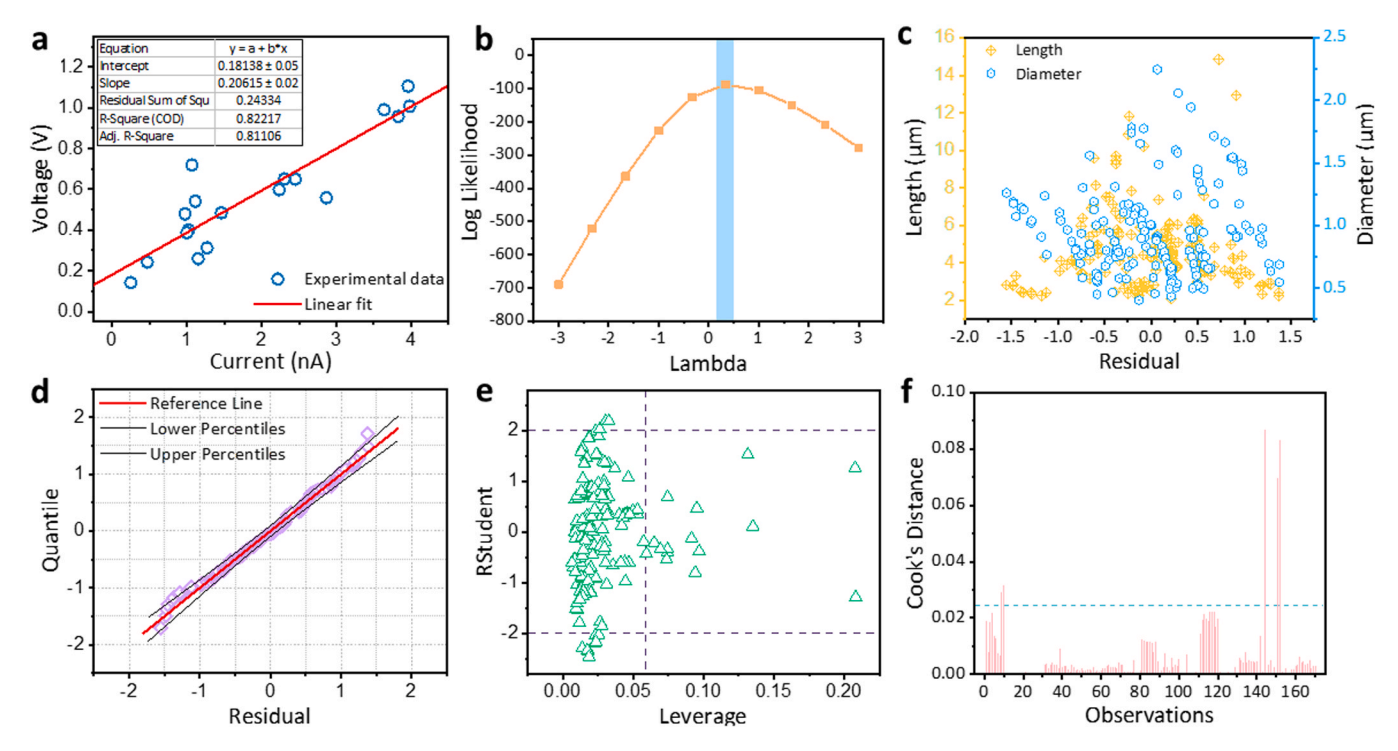


Fig. 3. (a) The relationship between the output voltages and the output currents. (b) The log-likelihood function values with different values of lambda. (c) The plots of residuals by length and diameter. (d) The normal Q-Q (quantile-quantile) plot. (e) The leverages versus studentized residuals. (f) The cook's distances of observations.

table are attached in Table S1 and Fig. S2. The regression model was analyzed based on the assumption that there are random errors in the experiments which follow the $N(0, \sigma^2)$ distribution [33]. It can be represented by residuals, which are the differences between the measured values and the predicted values. The residual plots show the spread of residuals graphically, helping to observe the distribution of residuals. The regression model is appropriate if the points in the residual plot are randomly dispersed around the horizontal axis. The residuals by length and diameter are shown in Fig. 3c as an example. The plots of residual by response variables and all regressors are shown in Figs. S3 and S4 to demonstrating the random distributions. The outliers can also be identified by the unusual points in the residual plots. Moreover, the normal Q-Q (quantile-quantile) plot of this model was shown in Fig. 3d to check the assumption of normality more accurately. The red reference line is a 45-degree line. The data points fall approximately along this reference line, indicating that the residuals are normally distributed. Further analysis was carried out to check the unusual and influential data. The leverages versus studentized residuals were plotted in Fig. 3e. Leverage is used to assess outliers with respect to the independent variables by identifying the observations that are distant from the predicted values [35]. High-leverage points can have outsized influences on the regression results. To further investigate the influential points, the cook's distances measuring the influence of the ith observation [36,37] are also calculated and plotted as Fig. 3f. The observations with a large cook's distance may strongly influence the fitted values of the model, and it should be taken into consideration when interpreting the results [38]. Although there are three points in our model that have relatively stronger cook's distances than other observations, the model did not change significantly if we remove the potential influential points. The equations to calculate the diagnostic statistics are listed in the Supporting Information. We can observe a few data points with relatively large values of these diagnostic statistics compared with other data points, which could be attributed to the nanowires grown randomly. The growth parameters of these special nanowires may not be controlled precisely as expected, leading to incompatible behaviors

between the growth parameters and measured outputs. Besides, we found that the length and diameter cannot be fully decoupled during the growth control, as shown in the scatterplots in Fig. S1. Such coupled interactions between these two variables lead to a narrower range of aspect ratios that can be achieved in the process. Therefore, the optimization process could be further improved with better control of growth parameters, more consistent growth, and more data points for new combinations of growth parameters and replications of involved conditions.

From our fitting model as per Eq. (4), we can find that the output current monotonically increases with higher growth density and aspect ratio of ZnO nanowire arrays. The ranges of growth parameters summarized from experimental data are density 0.03-0.75 counts µm⁻² length 2.0-9.0 µm, diameter 0.4-2 µm, and aspect ratio 1.5-15. Unlike the cases for density dependence, changes in current with lengths and diameters are not monotonic within the possible ranges, as shown in the scatterplots in Fig. S1. For instance, the output current reaches the maximum value when the length is 5.66 µm. Interestingly, this phenomenon does not agree with the previous works, which suggested that a longer length would be better [27]. It is possible that although longer length is theoretically beneficial for generating larger piezoelectric potential, the longer nanowires could not be vertically aligned as the shorter ones and may even be lodged on the substrates. Such a process could hinder the deformation of longer nanowires under the external force and reduce the effective output. Meanwhile, the output current reaches the minimum when the nanowire diameter is around 1.93 µm, close to the upper limit of the possible diameter range. However, the optimal conditions of all parameters suggested by the analytic solutions cannot be achieved simultaneously because of the correlations among parameters and experimental conditions' limitations. Thus, the finalized results from the model are length $\sim 4.83\,\mu m,$ diameter $\sim 0.43\,\mu m,$ aspect ratio ~ 11 , and density 0.73 counts μm^{-2} . The differences between the expected performances and the practical results appeared due to the limitations of traditional theoretical models. A theoretical model usually helps explain the phenomena of an object or a system based on developed principles with certain assumptions and boundary

conditions. However, the actual behaviors of the object or system do not strictly follow the theoretical assumptions owing to the restrictions in practice, such as the challenges in achieving perfectly homogeneous materials or absolute vacuum. The behavioral model developed by the data-driven method directly connects the observed performances with the production parameters, offering an effective approach to express the underlying impacts of production parameters. Furthermore, theoretical models rely on existed theories. At the same time, data-driven methods can be applied for exploring the relationships behind parameters without prior knowledge, suggesting the potential of the data-driven method in generating fundamental understandings of complex systems (e.g., manufacturing processes). Therefore, by combining the data-driven model with the possible ranges of growth parameters, we could determine the optimized structural parameters of ZnO nanogenerators with the improved outputs.

R. Wang et al.

The ZnO PENG with the optimized structural parameters (e.g., length $\sim 4.83\,\mu\text{m},$ diameter $\sim 0.43\,\mu\text{m})$ was integrated with a nanowire (Te nanowire) photosensor to demonstrate a self-powered nanosensor system [1]. The optical image of the photosensor is shown in Fig. 4a. A 405-nm laser diode was applied as the light source. The performances of the nanowire-based photosensor were characterized by different laser powers (Fig. 4b). The measured currents increased significantly with higher optical laser power. The photocurrent can be calculated by the equation [39]. In Fig. 4c, the derived photocurrents show good linearity across the applied optical power range without saturation. Afterward, the integrated nanosystem consisting of a ZnO nanogenerator and a Te-nanowire photosensor was fabricated and tested. The scheme for the system structure is shown in Fig. 4d. The ZnO nanogenerator was used to drive the operation of the tellurium nanowires based photosensor. When there was no light, the resistance of the sensor was about 1 M Ω . The corresponding current was ~1.14 nA (Fig. 4e). When the Te-nanowire photosensor was illuminated by the laser light, its resistance dropped

to 0.3 M Ω , and the corresponding current increased to 1.26 nA. The demonstrated self-powered nanosensor system can successfully detect the light illumination, suggesting the potential of optimized ZnO PENGs for powering the nanosensors. The self-powered nanosensor system is a prototypical demonstration of the knowledge learned from the data-driven method. Similar approaches can be applied in other systems whose performances are influenced by production parameters and are expected to have positive impacts in many fields, such as energy, sensors, and electronics [29].

3. Conclusion

In summary, we performed a systematic study and statistical analysis of the growth parameters' effects on the performances of ZnO PENGs. A behavioral model was estimated to build up the apparent connections between the output performance of PENGs and the production variables, including growth density, length, diameter, and aspect ratio of ZnO nanowires. The optimized ZnO PENGs suggested by this model were successfully integrated with a nanowire-based photosensor for the prototypical demonstration of a self-powered nanosystem. The gained knowledge in the fundamental process-property-performance relation through the presented data-driven learning method is critical for future scaled production of ZnO nanomaterials based devices and systems with optimized quality.

4. Experimental section

4.1. ZnO nanowires arrays preparation

ZnO nanowires samples were all grown by laser-induced hydrothermal synthesis at room temperature as described in the previous report [31]. Zinc chloride and hexamethylenetetramine (HMTA) (all

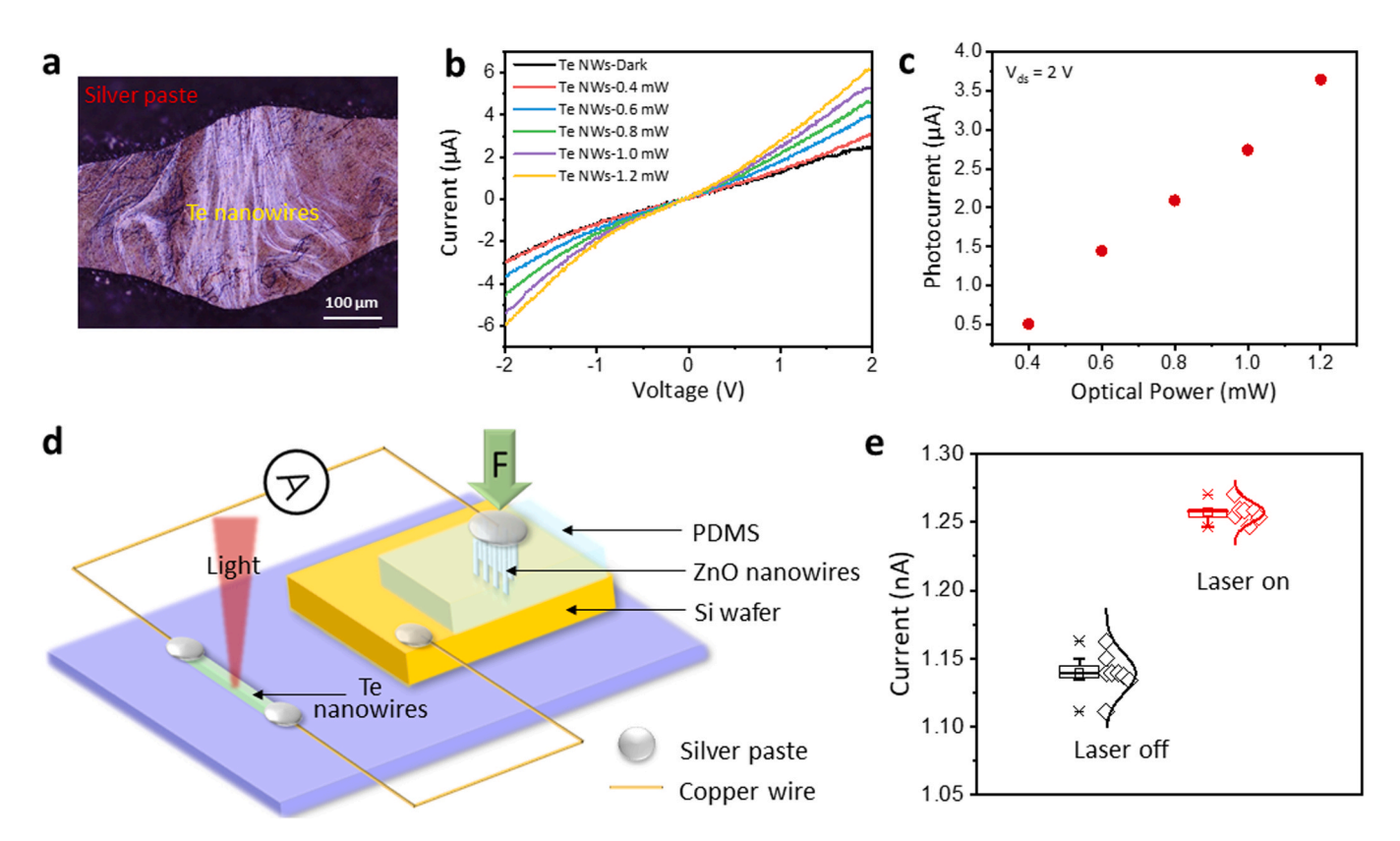


Fig. 4. Performances of self-powered nanosensor system. (a) The optical image of Te nanowires photosensor. (b) The photo-response of 405 nm laser from the Te nanowires photosensor. (c) The photocurrent versus optical powers from the Te nanowires photosensor. (d) The design scheme of a self-powered nanosystem with ZnO nanowires piezoelectric nanogenerator as the power source. (e) The current changes of the self-powered nanosystem with and without light illumination.

R. Wang et al. Nano Energy 83 (2021) 105820

chemicals from Sigma-Aldrich) were added into the water as the precursor solution. The substrates of Si were immersed into the precursor solution and irradiated by a ytterbium pulsed fiber laser to trigger the hydrothermal reaction. After growth, scanning electron microscopy (S. E.M., Hitachi 4800 Field-Emission) images were taken to measure the growth parameters from both top-down and cleaved cross-sectional views.

4.2. Fabrication of ZnO nanowires piezoelectric nanogenerators

A dielectric layer of polydimethylsiloxane (PDMS) was spin-coated with 3000 rpm/min for 5 min on the as-deposited ZnO nanowires arrays. They were cured at 70 $^{\circ}\text{C}$ for 15 min. Then, a silver paste was added on top of the PDMS layer as the top electrode covering the laser spot where ZnO nanowires are grown and connected with copper wires. An external force was applied by a linear motor (LinMot PS01–23 \times 80) to the PENG device. An electrometer (Keithley 6514) and a low current preamplifier (Stanford Research System, SR570) were employed to take the electrical measurements.

4.3. Statistical analysis

The regression model has the form

$$Y = \beta_0 + X\beta_1 + \epsilon, \tag{5}$$

where Y is the vector of responses, X is a matrix of the explanatory variables, β_0 and β_1 are the unknown coefficients to be estimated, and ϵ is a vector of random error terms with $N(0, \sigma^2)$ distribution. The method of least squares was employed to find the estimators of the regression parameters β_0 and β_1 , which is minimizing the squared error $\sum_{i=1}^n (Y_i - \beta_0 - \beta_1 X_i)^2$ [33]. The model was fitted through SAS® software, and the model assumptions were checked.

4.4. Self-powered nanosystems

Tellurium (Te) nanowires were synthesized by the hydrothermal method, as described in the previous report [40]. The as-synthesized Te nanowires were transferred on Si substrates with the coating of 300 nm SiO₂. The silver paste was applied on both ends of the Te nanowires along [0001] direction for electrical contacts under optical microscopy (Olympus BX-60). A focused laser beam (\approx 3 mm diameter) is illuminated over the device.

CRediT authorship contribution statement

Wenzhuo Wu: Conceived the idea. Wenzhuo Wu, C. Richard Liu: Supervised the project. Wenzhuo Wu, Ruoxing Wang: Designed the experiments. Siyu Liu: Prepared the ZnO nanowires samples by laser-induced hydrothermal synthesis and took the corresponding SEM images of the samples. Ruoxing Wang: Fabricated the PENG devices and conducted the PENG tests. Ruoxing Wang: Integrated the nanosensor system. Ruoxing Wang: Analyzed the data. Ruoxing Wang, Wenzhuo Wu: Wrote the manuscript. All authors have discussed the results and commented on the paper.

Declaration of Competing Interest

The authors declare that they have no known competing financial interests or personal relationships that could have appeared to influence the work reported in this paper.

Acknowledgments

Wenzhuo Wu and C. Richard Liu acknowledge the support from National Science Foundation (NSF) through the Grant CMMI-1663214.

Appendix A. Supporting information

Supplementary data associated with this article can be found in the online version at doi:10.1016/j.nanoen.2021.105820.

References

- [1] S. Xu, Y. Qin, C. Xu, Y. Wei, R. Yang, Z.L. Wang, Self-powered nanowire devices, Nat. Nanotechnol. 5 (2010) 366–373.
- [2] Z.L. Wang, J. Song, Piezoelectric nanogenerators based on zinc oxide nanowire arrays, Science 312 (2006) 242–246.
- [3] Z. Lin, B. Zhang, H. Guo, Z. Wu, H. Zou, J. Yang, Z.L. Wang, Super-robust and frequency-multiplied triboelectric nanogenerator for efficient harvesting water and wind energy, Nano Energy 64 (2019), 103908.
- [4] L. Huang, S. Lin, Z. Xu, H. Zhou, J. Duan, B. Hu, J. Zhou, Fiber-based energy conversion devices for human-body energy harvesting, Adv. Mater. 32 (2020), 1902034
- [5] F.-R. Fan, Z.-Q. Tian, Z.L. Wang, Flexible triboelectric generator, Nano Energy 1 (2012) 328–334.
- [6] Y. Yang, W. Guo, K.C. Pradel, G. Zhu, Y. Zhou, Y. Zhang, Y. Hu, L. Lin, Z.L. Wang, Pyroelectric nanogenerators for harvesting thermoelectric energy, Nano Lett. 12 (2012) 2833–2838.
- [7] X. Wang, Z.L. Wang, Y. Yang, Hybridized nanogenerator for simultaneously scavenging mechanical and thermal energies by electromagnetic-triboelectricthermoelectric effects, Nano Energy 26 (2016) 164–171.
- [8] M. He, Y.-J. Lin, C.-M. Chiu, W. Yang, B. Zhang, D. Yun, Y. Xie, Z.-H. Lin, A flexible photo-thermoelectric nanogenerator based on MoS2/PU photothermal layer for infrared light harvesting, Nano Energy 49 (2018) 588–595.
- [9] X. Wang, Piezoelectric nanogenerators—harvesting ambient mechanical energy at the nanometer scale, Nano Energy 1 (2012) 13–24.
- [10] C.-T. Huang, J. Song, W.-F. Lee, Y. Ding, Z. Gao, Y. Hao, L.-J. Chen, Z.L. Wang, GaN nanowire arrays for high-output nanogenerators, J. Am. Chem. Soc. 132 (2010) 4766–4771.
- [11] S. Xu, B.J. Hansen, Z.L. Wang, Nat. Commun. 1 (2010) 1-5.
- [12] C. Chang, V.H. Tran, J. Wang, Y.-K. Fuh, L. Lin, Direct-write piezoelectric polymeric nanogenerator with high energy conversion efficiency, Nano Lett. 10 (2010) 726–731.
- [13] J. Zhou, N.S. Xu, Z.L. Wang, Dissolving behavior and stability of ZnO wires in biofluids: a study on biodegradability and biocompatibility of ZnO nanostructures, Adv. Mater. 18 (2006) 2432–2435.
- [14] Z. Li, R. Yang, M. Yu, F. Bai, C. Li, Z.L. Wang, Cellular level biocompatibility and biosafety of ZnO nanowires, J. Phys. Chem. C 112 (2008) 20114–20117.
- [15] P. Yang, H. Yan, S. Mao, R. Russo, J. Johnson, R. Saykally, N. Morris, J. Pham, R. He, H.J. Choi, Controlled growth of ZnO nanowires and their optical properties, Adv. Funct. Mater. 12 (2002) 323–331.
- [16] X. Wang, Q. Li, Z. Liu, J. Zhang, Z. Liu, R. Wang, Low-temperature growth and properties of ZnO nanowires, Appl. Phys. Lett. 84 (2004) 4941–4943.
- [17] F. Wang, J.-H. Seo, G. Luo, M.B. Starr, Z. Li, D. Geng, X. Yin, S. Wang, D.G. Fraser, D. Morgan, Nat. Commun. 7 (2016) 1–7.
- [18] J.-H. Tian, J. Hu, S.-S. Li, F. Zhang, J. Liu, J. Shi, X. Li, Z.-Q. Tian, Y. Chen, Improved seedless hydrothermal synthesis of dense and ultralong ZnO nanowires, Nanotechnology 22 (2011), 245601.
- [19] J. Yeo, S. Hong, M. Wanit, H.W. Kang, D. Lee, C.P. Grigoropoulos, H.J. Sung, S. H. Ko, Rapid, one-step, digital selective growth of ZnO nanowires on 3D structures using laser induced hydrothermal growth, Adv. Funct. Mater. 23 (2013) 3316–3323.
- [20] J.B. In, H.J. Kwon, D. Lee, S.H. Ko, C.P. Grigoropoulos, In situ monitoring of laserassisted hydrothermal growth of ZnO nanowires: thermally deactivating growth kinetics, Small 10 (2014) 741–749.
- [21] D. Yang, Y. Qiu, Q. Jiang, Z. Guo, W. Song, J. Xu, Y. Zong, Q. Feng, X. Sun, Patterned growth of ZnO nanowires on flexible substrates for enhanced performance of flexible piezoelectric nanogenerators, Appl. Phys. Lett. 110 (2017), 063901
- [22] C.-L. Hsu, K.-C. Chen, Improving piezoelectric nanogenerator comprises ZnO nanowires by bending the flexible PET substrate at low vibration frequency, J. Phys. Chem. C 116 (2012) 9351–9355.
- [23] K.H. Kim, K.Y. Lee, J.S. Seo, B. Kumar, S.W. Kim, Paper-based piezoelectric nanogenerators with high thermal stability, Small 7 (2011) 2577–2580.
- [24] K.C. Pradel, W. Wu, Y. Ding, Z.L. Wang, Solution-derived ZnO homojunction nanowire films on wearable substrates for energy conversion and self-powered gesture recognition, Nano Lett. 14 (2014) 6897–6905.
- [25] Z. Li, G. Zhu, R. Yang, A.C. Wang, Z.L. Wang, Muscle-driven in vivo nanogenerator, Adv. Mater. 22 (2010) 2534–2537.
- [26] W. Wu, X. Wen, Z.L. Wang, Science (2013), 1234855.
- [27] R. Hinchet, S. Lee, G. Ardila, L. Montès, M. Mouis, Z.L. Wang, Performance optimization of vertical nanowire-based piezoelectric nanogenerators, Adv. Funct. Mater. 24 (2014) 971–977.
- [28] L. Serairi, D. Yu, Y. Leprince-Wang, Numerical modeling and simulation of ZnO nanowire devices for energy harvesting: numerical modeling and simulation of ZnO nanowire devices for energy harvesting, Phys. Status Solidi (C) 13 (2016) 683-687
- [29] Y. Wang, R.S.B. Ferreira, R. Wang, G. Qiu, G. Li, Y. Qin, D.Y. Peide, A. Sabbaghi, W. Wu, Data-driven and probabilistic learning of the process-structure-property

- relationship in solution-grown tellurene for optimized nanomanufacturing of highperformance nanoelectronics, Nano Energy 57 (2019) 480–491.
- [30] Z. Liu, S. Liu, W. Wu, C.R. Liu, The mechanism of controlled integration of ZnO nanowires using pulsed-laser-induced chemical deposition, Nanoscale 11 (2019) 2617–2623.
- [31] S. Liu, C.R. Liu, Morphology control by pulsed laser in chemical deposition illustrated in ZnO crystal growth, Cryst. Growth Des. 19 (2019) 2912–2918.
- [32] J.-T. Feng, Y.-P. Zhao, Experimental observation of electrical instability of droplets on dielectric layer, J. Phys. D Appl. Phys. 41 (2008), 052004.
- [33] M.H. Kutner, C.J. Nachtsheim, J. Neter, W. Li, Applied Linear Statistical Models, McGraw-Hill,, Irwin New York, 2005.
- [34] K.C. Singh, Basic Physics, PHI Learning Pvt. Ltd.,, 2009.
- [35] X. Liu, Methods and Applications of Longitudinal Data Analysis, Elsevier,, 2015.
- [36] C. Kim, Y. Lee, B.U. Park, Cook's distance in local polynomial regression, Stat. Probab. Lett. 54 (2001) 33–40.
- [37] R.D. Cook, Detection of influential observation in linear regression, Technometrics 19 (1977) 15–18.
- [38] J. Fox, Regression Diagnostics Vol. 79: An Introduction, SAGE Publications Incorporated, 1991.
- [39] W. Wu, L. Wang, R. Yu, Y. Liu, S.H. Wei, J. Hone, Z.L. Wang, Piezophototronic effect in single-atomic-layer MoS2 for strain-gated flexible optoelectronics, Adv. Mater. 28 (2016) 8463–8468.
- [40] Y. Wang, R. Wang, S. Wan, Q. Wang, M.J. Kim, D. Ding, W. Wu, Scalable nanomanufacturing and assembly of chiral-chain piezoelectric tellurium nanowires for wearable self-powered cardiovascular monitoring, Nano Futures 3 (2019), 011001.



Ruoxing Wang received her BS degree in Chemistry in 2011 from University of Science and Technology of China (USTC). She is currently a PhD student in Industrial Engineering at Purdue University under the supervision of Prof. Wenzhuo Wu. Her research interests mainly focus on nanomanufacturing including the design of functional nanomaterials and fabrication of nanodevices for energy and human-health related applications.



Dr. Siyu Liu received her BS degree in Materials Science and Engineering in Shanghai Jiao Tong University in 2014, and MS degrees in Industrial Engineering and Environmental Engineering from Purdue University and Fudan University in 2015 and 2017. Dr. Liu received her PhD from Purdue University in Industrial Engineering in 2020. Dr. Liu's research interests include laser-induced manufacturing, focusing on developing a method of controlled selective growth of nanomaterials by pulsed-laser activated chemical synthesis and exploring fundamental theories of crystallization.



Dr. Richard Chunghorn Liu is the Professor Emeritus in the School of Industrial Engineering at Purdue University. A graduate of National Cheng Kung University, Liu earned his master's degree at the University of Cincinnati and doctorate at Purdue. After starting his academic career at Stanford, he joined Purdue's faculty in 1978, where he served as a full professor since 1985. He has published over 180 peer reviewed research papers, holds three patents and taught courses on Design, Manufacturing and Competitive Strategies for Products and Processes. In the last ten years of his career, Dr. Liu has worked in additive manufacturing and nanomanufacturing.



Dr. Wenzhuo Wu is the Ravi and Eleanor Talwar Rising Star Assistant Professor in the School of Industrial Engineering at Purdue University. He received his B.S. degree in Electrical Engineering from University of Science and Technology of China (USTC) in 2005, and M.S. degree in Electrical Engineering from National University of Singapore (NUS) in 2008. Dr. Wu received his Ph.D. from Georgia Tech in Materials Science and Engineering in 2013 under the supervision of Prof. Zhong Lin Wang. Dr. Wu's research interests include design, manufacturing, and integration of nanomaterials for applications in energy, electronics, quantum technologies, and wearable devices.